

Metal or Nonmetal Cooperation with a Phenyl Group: Route to Catalysis? A Computational Investigation

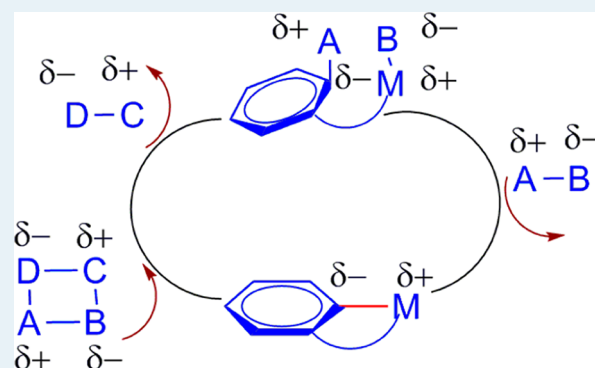
Kamalika Ghatak, Manoj Mane, and Kumar Vanka*

Physical Chemistry Division, National Chemical Laboratory (CSIR), Dr. Homi Bhabha Road, Pashan, Pune, Maharashtra –411008, India

Supporting Information

ABSTRACT: Full quantum mechanical calculations demonstrate that cooperativity in the form of the activation of the M–C bond (M: transition metal or boron, C: the ipso carbon of the coordinated phenyl group) can lead to effective catalysis pathways. Calculations show that the presence of an aromatic bidentate ligand attached to a transition metal, or even a main group element, such as boron, can lead to effective catalysts for a range of important reactions, such as the dehydrogenation of ammonia borane and formic acid and the activation of the N–H bond in aromatic amines. Moreover, it is shown that the design of tridentate pincer complexes with the aromatic group at a terminal end can lead to effective M–C cooperativity. As such, the current work introduces a new concept in cooperativity and bond activation chemistry.

KEYWORDS: metal–ligand cooperativity, catalysis, density functional theory, small molecule activation



1. INTRODUCTION

Non oxidative addition and elimination reactions using organometallic complexes that demonstrate metal–ligand cooperativity are of great practical significance, especially if the reactions can occur reversibly over a small span of time. Complexes having tridentate “pincer ligands”, such as PCP [$C_6H_3(R')(P(R)_3CH_2)_2-1,2,6$], POCOP [$C_6H_3(R')(P(R)_3O)_2-1,2,6$], NCN [$C_6H_3(R')(N(R)_2CH_2)_2-1,2,6$], PCN [$C_6H_3((R'')P(R)_3CH_2)(N(R')_2CH_2)-1,2,6$], PNP [$C_5H_3N(R)-(P(R')_3CH_2)_2-1,2,6$], and others,^{1,2} have proved to be very versatile and effective ligands in facilitating such reactions in conjunction with transition metals such as iridium, platinum, rhodium, osmium, and ruthenium. The group of David Milstein has exploited the cooperativity between the metal and pincer ligands to obtain a stable platinum oxo complex exhibiting interesting reactivity³ and to split water and obtain molecular oxygen and hydrogen.⁴ Ahuja et al.⁵ have used different pincer-ligated iridium complexes to convert linear alkanes to aromatic compounds. Pincer ligand-coordinated organometallic complexes have also been effective at N–H, N–C, C–C, C–H, H–H, N–H, and O–H activation.^{6–8,2} Such complexes have been also been found to be important for reactions such as the highly efficient dehydrogenation of ammonia borane as a result of the hemi-labile nature of the nitrogen–metal bond.⁹

The rich and varied chemistry that has emerged from the effective use of pincer ligand complexes gives reason to believe that further exploitation of metal–ligand cooperativity using such complexes is likely in the near future. However, it is interesting to note that cooperativity between the metal center and a coordinated carbon atom in pincer ligand complexes has

not been explored. To the best of our knowledge, the only reported example of the non-innocent behavior of a metal–carbon bond in a pincer complex is by Musa et al.¹⁰ for $C(sp^3)$ metalated pincer compounds. Moreover, the reactions that were studied with this complex were found to require a significant amount of time and needed extra heating over a period of 12 h to ensure completion. In addition, to date, no pincer-ligated metal complexes having an aromatic group as one of the arms of the pincer have been reported to display metal– $C(sp^2)$ cooperativity through activation of the metal–ipso carbon bond.

We postulate here that the reason pincer ligand-containing complexes do not exhibit metal–carbon cooperativity is because of the steric constraints imposed by the tridentate nature of the ligand coordination and, further, that employing analogous aromatic bidentate ligands in place of the tridentate pincer ligands (see Figure 1), or tridentate pincers where the phenyl ring is at a terminal end of the ligand, would reduce the steric restrictions. This would serve to make the bidentate or tridentate complexes efficient catalysts because of the emergence of cooperativity between the metal and the ipso



Figure 1. Tridentate and bidentate aromatic ligand complexes.

Received: March 5, 2013

Revised: March 22, 2013

Published: March 27, 2013

carbon of the attached phenyl group. An example for such a possibility is shown in Figure 2, where the catalysis of

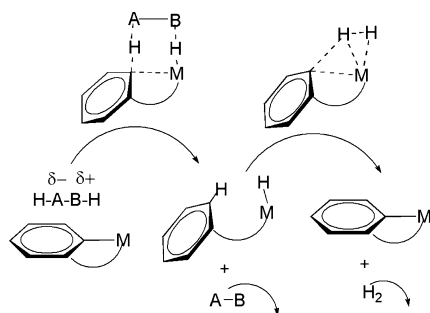


Figure 2. The catalysis of dehydrogenation reactions through the use of metal–ipso carbon cooperativity in aromatic bidentate complexes.

dehydrogenation reactions is discussed, for a complex with an aromatic bidentate ligand coordinated to the metal center. The dehydrogenation would proceed with the loss of two hydrogen atoms from the substrate molecule $\text{H}-\text{A}-\text{B}-\text{H}$, with the protic hydrogen being taken up by the ipso carbon of the phenyl ring and the hydridic hydrogen forming a bond with the metal center (see Figure 2). Following this, the oxidative metalation step would complete the catalytic cycle, releasing hydrogen gas, H_2 , and regenerating the original catalyst species. The facile activation of the metal–ipso carbon bond would make the first step kinetically and thermodynamically favorable, and the likely ready re-coordination of the phenyl ring back to the metal center in the second step would complete the cycle. Likewise, analogous to the dehydrogenation reaction discussed in Figure 2, one could envisage other possible reactions that could be effectively catalyzed by the use of the aromatic bidentate complexes or tridentate complexes having the phenyl ring at a terminal end and not at the center.

The reason the catalytic pathway, illustrated in Figure 2, involving metal–carbon activation has been considered for aromatic ligands and not for their aliphatic analogues, is because of the possibility of an agostic interaction between the $\text{C}(\text{sp}^2)-\text{H}$ bond and the metal, as experimentally observed and reported in several complexes containing an aromatic ligand.^{11–15} Such an interaction would pre-activate the $\text{C}(\text{sp}^2)-\text{H}$ bond in this step and thus aid in reducing the barrier to metalation, thereby ensuring the efficiency of the catalysis process.

The effectiveness of the proposed metal–carbon cooperative catalytic pathway will be demonstrated in the Results and Discussion section by considering the example of the tridentate pincer ligand complex: $(\text{POCOP})\text{IrH}_2$, one of the most efficient catalysts for dehydrogenating ammonia borane¹⁶ (AB). It will be shown that the bidentate analogue of the tridentate $(\text{POCOP})\text{IrH}_2$, if synthesized (“ $(\text{POC})\text{IrH}_2$ ”), would be considerably more effective at catalyzing the same reaction. We will also demonstrate computationally that employing tridentate ligands with the aromatic ring at the terminal end would also lead to the emergence of metal–carbon cooperativity. The potential of metal–carbon cooperativity in bidentate complexes will be further discussed for other cases, such as the experimentally synthesized real system: $\text{Ta}(\text{=CH}-t\text{-Bu})[\text{C}_6\text{H}_3(\text{CH}_2\text{NMe}_2)_2-2,6](\text{Cl})(\text{O}-t\text{-Bu})$ and even for non-metal based complexes, such as $\text{B}(\text{Et})[\text{C}_6\text{H}_4(\text{CH}_2\text{CH}_2)]$. Moreover, it will be shown that the catalysis of other important reactions, such as the dehydrogenation of formic acid, as well as

the activation of the $\text{N}-\text{H}$ bond in aromatic amines, will become feasible through the proposed route of metal–carbon cooperativity.

2. RESULTS AND DISCUSSION

2.1. Comparison of AB Dehydrogenation Using Bidentate and Tridentate Iridium Catalysts. The pincer ligand containing complex, $(\text{POCOP})\text{IrH}_2$, has been found to be a very efficient catalyst for the dehydrogenation of ammonia borane: NH_3BH_3 (AB).¹⁶ The structure of $(\text{POCOP})\text{IrH}_2$ is shown in Figure 3. Ammonia borane, it may be noted, is one of

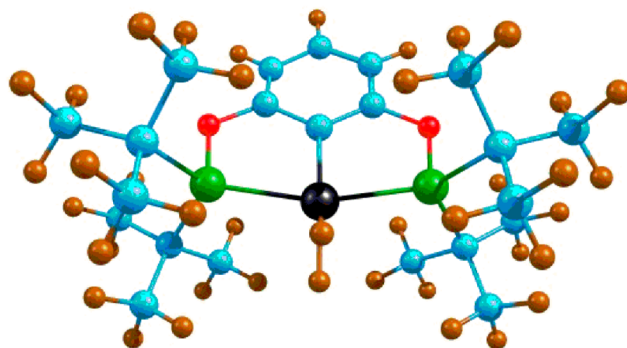


Figure 3. Structure of tridentate $(\text{POCOP})\text{IrH}_2$ pincer catalyst; the color scheme is as follows: iridium, black; carbon, blue; phosphorus, green; oxygen, red; and hydrogen, brown.

the most promising candidates for the chemical storage of hydrogen,¹⁷ and therefore, the efficient catalysis of AB dehydrogenation is an important problem in hydrogen storage research. The mechanism for the dehydrogenation of AB using the $(\text{POCOP})\text{IrH}_2$ catalyst has been reported by Paul and Musgrave.¹⁸ As shown in Figure 4, the Paul–Musgrave

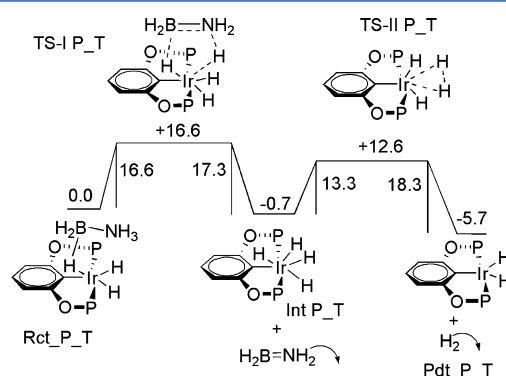


Figure 4. The free energy profile for the Paul–Musgrave reaction pathway for the dehydrogenation of ammonia borane by the $(\text{POCOP})\text{IrH}_2$ catalyst; all energies are in kcal/mol.

dehydrogenation mechanism proceeds through the coordination of AB to the $(\text{POCOP})\text{IrH}_2$ catalyst, followed by removal of NH_2BH_2 from the vicinity of the catalyst. The $(\text{POCOP})\text{IrH}_4$ intermediate thus formed is then converted to the $(\text{POCOP})\text{IrH}_2$ catalyst by the loss of H_2 , thereby completing the catalytic cycle.¹⁸ The competing pathway for the $(\text{POCOP})\text{IrH}_2$ catalyst, involving the proposed metal–carbon cooperativity, is shown in Figure 5. This pathway is found not to compete, having a slowest step barrier that is higher by 14.5 kcal/mol than the slowest step of the Paul–Musgrave pathway.

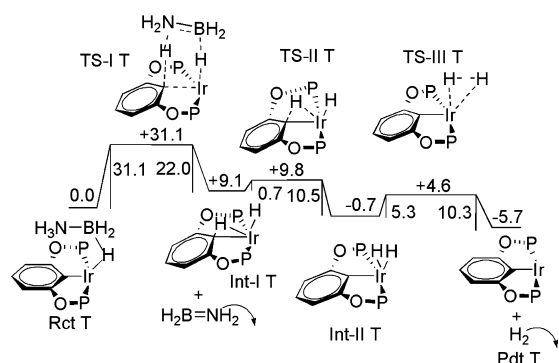


Figure 5. The free energy profile for the dehydrogenation of ammonia borane through the proposed M–C activation pathway for the (POCOP)IrH₂ catalyst; all values are in kcal/mol.

However, it is likely that the metal–ligand cooperative pathway might become more competitive if the steric restrictions, imposed by the tridentate nature of the bonding of the ligand at the metal center, could be reduced. This would be possible if the catalyst employed were to have an *aromatic bidentate ligand coordination to begin with*. This point is underlined through calculations with the bidentate analogue of (POCOP)IrH₂: the “(POC)IrH₂” complex. The optimized structure for (POC)IrH₂ is shown in Figure 6: the complex has

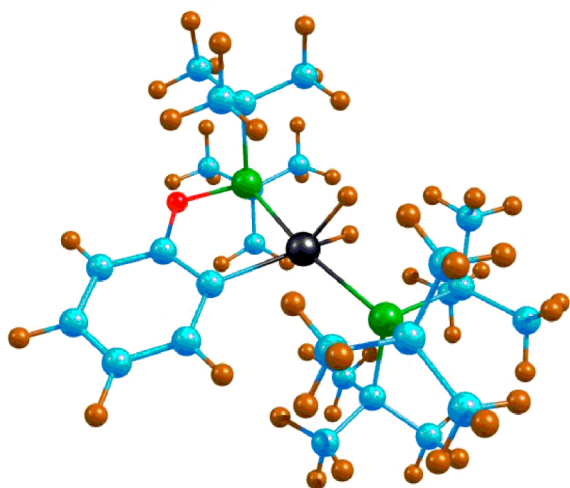


Figure 6. The optimized geometry of the iridium bidentate complex: (POC)IrH₂ complex; the color scheme is the same as in Figure 3.

a monodentate phosphine (with tertiary butyl groups), and a bidentate ligand with an aromatic ring as one of the arms and a phosphine as the other, of the bidentate ligand. The fact that this system would be stable in solution was confirmed through calculations investigating the dissociation of the phosphine from this complex and the replacement of the same with a solvent (THF) molecule. As shown in Figure S1 of the Supporting Information, it was found that such a reaction would be highly unlikely, being endothermic by 104.8 kcal/mol. Hence, the complex (POC)IrH₂ would be stable in solution.

For this system, the catalysis of AB dehydrogenation would prefer the pathway of metal–ipso carbon cooperativity, as is made clear from Figures 7 and 8. The slowest step barrier for the reaction, 15.3 kcal/mol, through the proposed metal–ipso carbon cooperative pathway, is lower by 1.6 kcal/mol than the

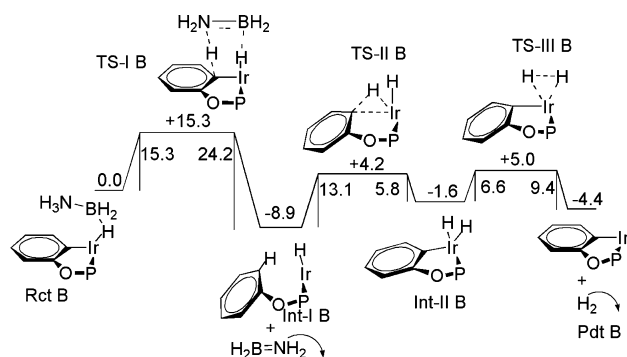


Figure 7. The free energy profile for the proposed M–C activation pathway for the dehydrogenation of ammonia borane by the (POC)IrH₂ catalyst; all energies are in kcal/mol.

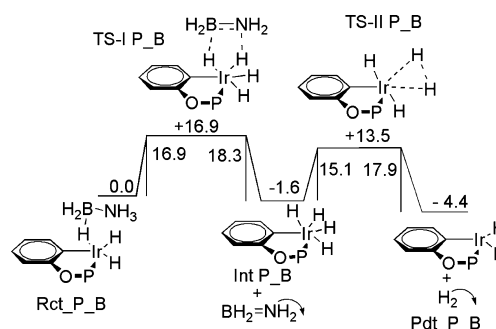


Figure 8. The free energy profile for the dehydrogenation of ammonia borane through the Paul–Musgrave pathway for the (POC)IrH₂ catalyst; all energies are in kcal/mol.

slowest step for the Paul–Musgrave pathway in this case, and lower by 1.3 kcal/mol than the slowest step barrier (16.6 kcal/mol) for the Paul–Musgrave pathway obtained for the tridentate iridium analogue. These computational results therefore underline the potential of metal–carbon cooperativity, which is dormant in the pincer ligand complex but is unlocked in the bidentate analogue.

The reasons the bidentate catalyst is determined to be more effective than the corresponding tridentate complexes are 2-fold: (i) the reduction of steric hindrance for the motion of the phenyl ring out of the POC plane, and (ii) the low barrier for the second transition state because of the pre-activation of the ipso carbon–hydrogen bond due to the aromatic agostic interaction of the bond with the iridium metal center. There have been experimental reports in the literature that have hypothesized the existence of such an interaction for rhodium^{11–13} and ruthenium metal^{14,15} complexes. The presence of the aromatic agostic interaction in the (POC)IrH₂ complex is made evident from the geometric features obtained for the intermediate: **Int-I B** (see Figure 7) along the catalytic path. The structure of **Int-I B** is shown in Figure 9 below. The ipso carbon–hydrogen bond length in **Int-I B** is found to be 1.12 Å, which is greater than the standard aromatic C–H bond length (1.09 Å). Moreover, the hydrogen of the pre-activated C–H bond is found to lie out of the plane of the aromatic ring by 11.25°. Furthermore, the Ir–H distance is found to be 2.10 Å, and the Ir–H–C angle is observed to be 116.81°, both falling in the range of typical agostic interactions. To further underline the agostic nature of the interaction, another conformer of **Int-I B**, **Int-I B'** was optimized, having the aromatic ring turned away from the iridium metal center,

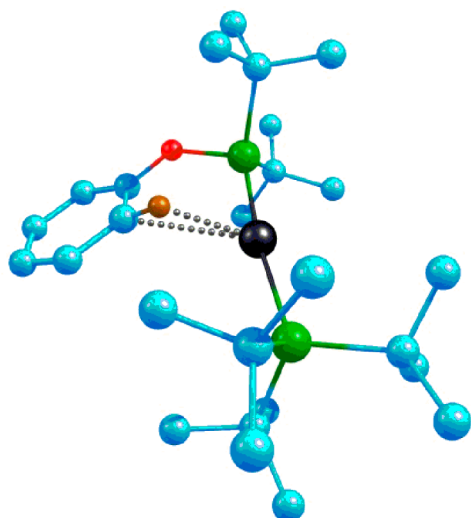


Figure 9. The optimized structure of **Int-IB**, the hydrogenated (POC)IrH₂ catalyst. The color scheme is the same as in Figure 3. Only the hydrogen coordinated to the ipso carbon is shown; the rest of the hydrogens have been removed for the purpose of clarity.

thereby denying the system the possibility of an aromatic agostic interaction. The two conformers, **Int-I B** and **Int-I B'** are shown juxtaposed in Figure S4 of the Supporting Information. As the figure shows, **Int-I B'** is less stable by 8.1 kcal/mol (ΔE) than **Int-I B**, providing further evidence of the stabilizing influence of the aromatic agostic interaction in **Int-I B**. Hence, the cumulative evidence points to the pre-activation of the C(sp²)-H bond, which provides the explanation as to why the second barrier (the barrier for the oxidative metalation step) is 13.1 kcal/mol, thereby making the catalytic cycle a feasible process.

It is also interesting to note that an aromatic agostic interaction with the metal center is more likely than an aliphatic agostic interaction: no structural evidence for an agostic interaction is observed in the optimized complex Ir(H)₃[P(CH₃)₃][P(Me)₃OCH₂CH₂(CH₃)], a structure (shown in Figure S5 of the Supporting Information) in which the aromatic phenyl ring has been replaced with an aliphatic CH₂CH₂ group. Thus, the corresponding metalation step for the aliphatic complex has been calculated to be 23.4 kcal/mol (ΔE value), higher than the corresponding step in the aromatic complex by 9.6 kcal/mol (ΔE value). These investigations therefore reveal that the bidentate complexes would be more effective for aromatic ligands, and not for their aliphatic analogues.

The results discussed in this section therefore indicate that the iridium bidentate complex, (POC)IrH₂, if synthesized, would be a more effective catalyst for ammonia borane (AB) dehydrogenation than the tridentate complex, (POCOP)IrH₂, because of Ir-*ipso* carbon cooperativity, discussed here, for the bidentate complex, which gives it an edge over the original mechanism, described by Paul and Musgrave for the tridentate complex.¹⁸ This computational demonstration of the potential for metal-carbon cooperativity in bidentate complexes can lead to significant improvements in catalyst design for important chemical transformations.

It is important to mention here that it may also be possible to observe metal-carbon cooperativity in tridentate pincer ligand complexes. This would be possible if the steric constraints were

to be reduced by the putting of the aromatic phenyl ring at the terminal end of the ligand instead of in the center. An example of a model tridentate pincer ligand with such a linkage is shown in Figure 10. The ligand coordinated to the iridium center has

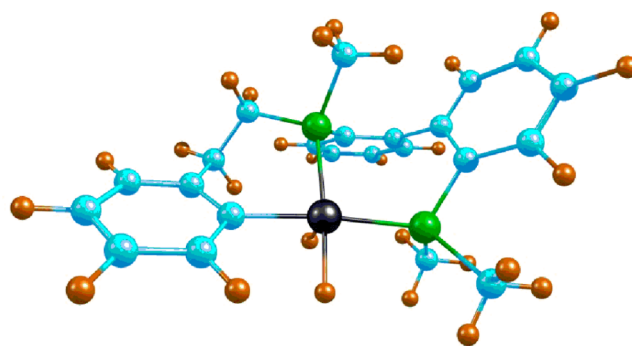


Figure 10. The optimized geometry of (PPC)IrH₂ complex; the color scheme is the same as in Figure 3.

two consecutive phosphine linkages, followed by a phenyl linkage. This ligand is henceforth termed as “PPC”; thus, the complex would be (PPC)IrH₂. This complex would provide a “bidentate” environment to the phenyl ligand and, thus, could allow the emergence of metal-carbon cooperativity. This is further illustrated by doing AB dehydrogenation catalysis with this (PPC)IrH₂. As Figures 11 and 12 indicate, the metal-

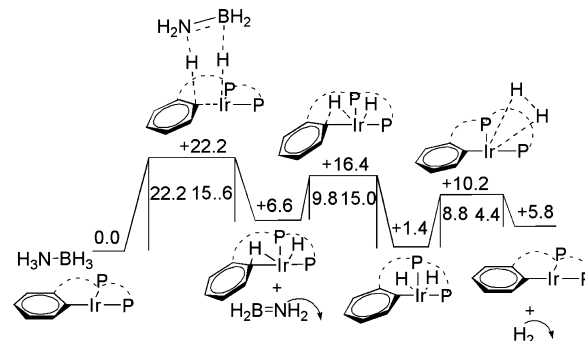


Figure 11. The free energy profile for the proposed M-C activation pathway for the dehydrogenation of ammonia borane by a (PPC)IrH₂ complex; all energies are in kcal/mol.

carbon activation pathway (slowest step barrier: 22.2 kcal/mol) is seen to be competitive in comparison to the Paul-Musgrave

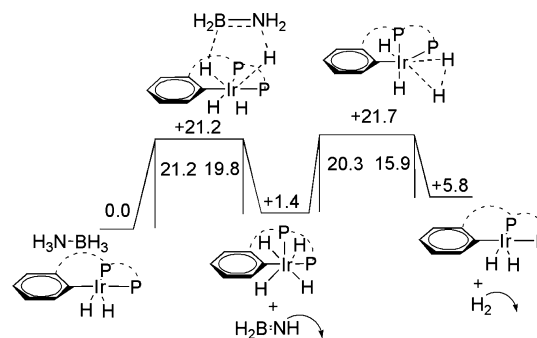


Figure 12. The free energy profile for the Paul-Musgrave pathway for the dehydrogenation of ammonia borane by a (PPC)IrH₂ complex; all energies are in kcal/mol.

pathway (slowest step barrier: 21.2 kcal/mol). Tridentate pincer ligand complexes having the phenyl ring at a terminal end, instead of in the center, have already been prepared.¹⁹ The current work therefore provides an example of the potential of such complexes for catalysis. The focus of the remainder of the paper, however, is on aromatic bidentate ligand complexes.

Since there already exist metal complexes having aromatic bidentate ligands, they can be considered candidates for the catalysis processes. The next section focuses on one such existing complex: the bidentate tantalum-based carbene complex, Ta(=CH-*t*-Bu)[C₆H₃(CH₂NMe₂)₂-2,6](Cl)(O-*t*-Bu), and shows how this complex could potentially display metal-carbon cooperativity.

2.2. AB Dehydrogenation Using a Bidentate Tantalum Catalyst. The Ta(=CH-*t*-Bu)[C₆H₃(CH₂NMe₂)₂-2,6](Cl)(O-*t*-Bu) (Ta-*bid*) complex, synthesized in 1997,²⁰ is considered in this section for the catalysis of the AB dehydrogenation reaction. This is a carbene complex, and it is likely that in the presence of a hydrogenating agent such as ammonia borane, the first reaction that would occur is the hydrogenation of the Ta-carbene double bond, rather than the activation of the metal-*ipso* carbon bond of the coordinated aromatic ring. Calculations done with a model system (shown in Figure S6 of the Supporting Information) bear out this view. However, because the hydrogenation of the Ta=C bond would lead to a stable product (the product is found to be 8.6 kcal/mol more stable than the reactants for the model system), the hydrogenated species is likely to be long-lasting in the reaction vessel and can therefore act as the catalyst for ammonia borane dehydrogenation. The optimized structure of the hydrogenated form of the real system, Ta(H)(CH₂-*t*-Bu)[C₆H₃(CH₂NMe₂)₂-2,6](Cl)(O-*t*-Bu), Ta-*bid*-H₂, is shown in Figure S7 of the Supporting Information. As shown in Figure 13, calculations done with Ta-*bid*-H₂ indicate that

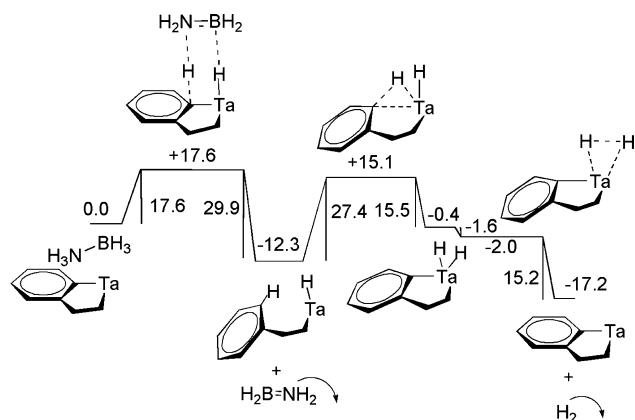


Figure 13. The free energy profile for the proposed M-C activation pathway for the dehydrogenation of ammonia borane by a tantalum complex; all energies are in kcal/mol.

the barriers for the dehydrogenation process are comparable to the bidentate iridium catalyst case. These results thus indicate that complexes that have already been synthesized may become active and efficient catalysts for this important dehydrogenation reaction.

2.3. AB Dehydrogenation Using a Boron Complex. We have also considered the interesting possibility of *nonmetal complexes with an aromatic bidentate linkage* also proving to be effective at catalysis processes through the proposed cooper-

ativity pathway. The complex that has been considered for this is the boron containing molecule, B(Et)[C₆H₄(CH₂CH₂)] (B-*cat*). It is to be noted that the analogous complex, B(Pr)[C₆H₄(CH₂CH₂)],²¹ has already been synthesized, and therefore, the synthesis of B(Et)[C₆H₄(CH₂CH₂)] should be feasible.

There are several excellent reasons for investigating boron-containing complexes:

- Like metal centers, boron is also known to be acidic, and so would be susceptible to attack from a complex of the type HABH, shown earlier in Figure 2.
- The second step, which involves the elimination of hydrogen, H₂, from the complex to complete the cycle, requires the increase in coordination number at the acidic center. Like transition metals, boron, too, has displayed the ability to increase its coordination number by two units.^{22,23}
- A further motivation is the need to develop nonmetal-based catalyst systems for important reactions, such as ammonia borane dehydrogenation. Nonmetal catalyst systems are likely to be less toxic, and therefore more environmentally friendly, as well as less expensive, than their metal analogues.²⁴ A phosphorus-based analogue of pincer-ligated transition metal complexes has recently been prepared,²⁵ for instance, and is considered a promising harbinger for future work in preparing nonmetal analogues to transition metal complexes.²⁶

Keeping these factors in mind, the complex B-*cat* was considered for the AB dehydrogenation process. As Figure 14 shows, the catalysis cycle contains two barriers of 35.9 and 30.9 kcal/mol, respectively.

A further advantage of investigating the nonmetal boron complex is that the relative smallness of its size, in comparison with the larger, metal-containing complexes, allows for further computational investigations that would be prohibitively expensive computationally for the metal-based systems. Hence, for the boron complex, the effect of modification of

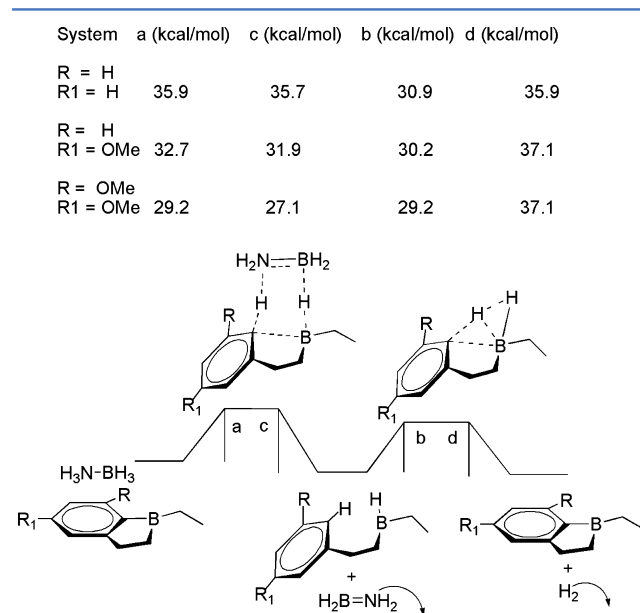


Figure 14. The free energy profile for the proposed M-C activation pathway for the dehydrogenation of ammonia borane by boron complexes; all energies are in kcal/mol.

the catalyst by the addition of functional groups has also been considered. Electron-donating OCH_3 groups were added at the ortho and para positions of the complex, and this was found to lead to a reduction of the barriers by 6.7 kcal/mol (see Figure 14). These calculations also suggest that the efficiency of the catalysts can be further improved by suitable addition of functional groups, not only for the case of the boron complex considered here, but also, by extension, for the previous metal-based complexes.

It is true that the barrier heights discussed here for the boron systems are still higher than those obtained in the iridium and tantalum cases considered earlier. However, it is to be noted that current effective main-group catalyst systems have been found to function well only at higher temperatures ($80\text{ }^\circ\text{C}$ for the phosphorus-based system mentioned above²⁵) and have been seen to have high barriers, ranging from 29.1 to 44.3 kcal/mol^{27–29} during the catalysis process. Hence, the obtained values for the boron systems investigated here can be considered respectable, especially for the OCH_3 -substituted case.

2.4. Other Reactions with the Bidentate (POC)IrH₂ complex: Dehydrogenation of Formic Acid and N–H Activation. The previous section discussed the potential of bidentate complexes in catalyzing the dehydrogenation of ammonia borane, an important reaction because of its relevance in the chemical storage of hydrogen.¹⁷ It is also likely that the lability of the metal–carbon bond in bidentate complexes can be exploited for other important reactions, as well. In this section, we discuss two such possibilities: the catalysis of the dehydrogenation of formic acid (HCOOH), and the activation of the N–H bond in aromatic amines. The bidentate complex considered for these cases is the (POC)IrH₂ complex.

The dehydrogenation of formic acid has assumed importance recently because of the recognition of its potential for the chemical storage of hydrogen,³⁰ with HCOOH having an additional advantage in that its regeneration after dehydrogenation would be a very facile process.³⁰ A complex that can catalyze the ready removal of hydrogens from HCOOH to yield CO_2 can thus be of great importance. We discuss here the possibility of the (POC)IrH₂ complex acting as a homogeneous catalyst to dehydrogenate HCOOH . Shown in Figure 15 is the potential energy surface for the dehydrogenation process. The three barriers corresponding to (a) the removal of the hydridic and the protic hydrogens from the carbon and oxygen atoms of HCOOH respectively, (b) the transfer of hydrogen from the ipso carbon of the aromatic ring to iridium and (c) the

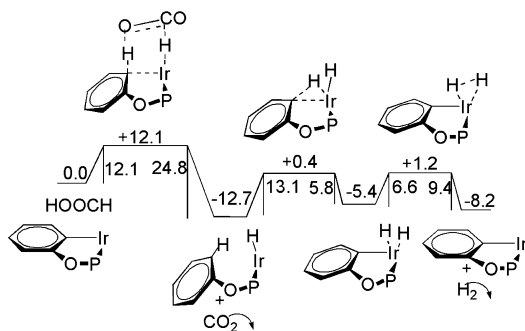


Figure 15. The free energy profile for the proposed M–C activation pathway for the dehydrogenation of formic acid by the (POC)IrH₂ complex; all energies are in kcal/mol.

subsequent removal of the hydrogens from the catalyst are 12.1 and 13.1 kcal/mol and 6.6 kcal/mol. These values are significantly lower than those obtained for systems employing the most efficient catalysts for ammonia borane dehydrogenation,^{9,16,31} which suggests that bidentate ligand-containing catalysts that can exploit metal–carbon cooperativity have great potential to be excellent catalysts for dehydrogenating HCOOH .

The N–H activation of amines by metal complexes is a process that has not been widely studied, despite its potential importance in explaining a range of important metal catalyzed transformations.^{32–42} Recently, Milstein's group has reported the N–H activation of aromatic amines such as $\text{C}_6\text{H}_3\text{Cl}_2\text{NH}_2$, using the concept of metal–ligand cooperativity involving pincer ligand complexes and aromatization–dearomatization.^{43,44} To test the efficacy of the metal–ipso carbon cooperativity for N–H bond activation, calculations were performed with the (POC)IrH₂ catalyst, and the N–H activation in $\text{C}_6\text{H}_3\text{Cl}_2\text{NH}_2$ was studied. As shown in Figure 16, the barrier for the N–H activation was found to be 23.4 kcal/mol, which indicates that such a process would be feasible at ambient temperature.

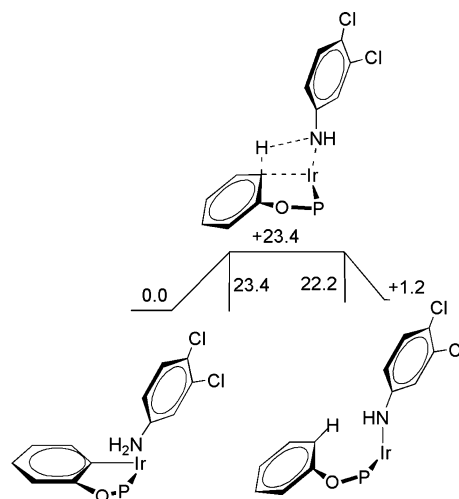


Figure 16. The free energy profile for the proposed M–C pathway for the activation of the N–H bond in $\text{C}_6\text{H}_3\text{Cl}_2$.

3. CONCLUSIONS

The current work, employing full quantum mechanical (QM) density functional theory (DFT) methods, demonstrates the potential of aromatic bidentate metal and nonmetal complexes, as well as of tridentate pincer complexes having the aromatic linkage at a terminal end, to act as catalysts for important chemical reactions. It has been shown that such systems may be even more effective than the currently employed tridentate pincer ligand complexes, due to the possibility, absent in the currently employed pincer complexes, of exploiting metal–carbon cooperativity. What has also been shown is that metal–carbon cooperativity can be exploited in a range of different complexes, both metal and, significantly, nonmetal, for catalyzing a variety of reactions, including ammonia borane dehydrogenation, formic acid dehydrogenation, and N–H activation. Therefore, metal (or nonmetal)–ipso $\text{C}(\text{sp}^2)$ cooperativity, which has been discussed for the first time in

this work, represents an important new avenue for achieving important chemical transformations.

4. COMPUTATIONAL DETAILS

All the DFT calculations were carried out using the Turbomole 6.0 suite of programs.⁴⁵ Geometry optimizations were performed using the Becke Perdew 86 (BP-86) functional.^{46,47} The electronic configuration of the atoms was described by a triple- ζ basis set augmented by a polarization function (Turbomole basis set TZVP).⁴⁸ The basis set employed for iridium includes relativistic effective core potentials (recps). The resolution of identity (ri),⁴⁹ along with the multipole accelerated resolution of identity (marij)⁵⁰ approximations were employed for an accurate and efficient treatment of the electronic Coulomb term in the density functional calculations. Since it is possible that the geometry optimization procedure with DFT may be sensitive to the nature of the functional, a further test has been done to ensure the reliability of the obtained geometry optimized structures: all the minima and transition state structures were also optimized with the Perdew, Burke, and Erzenhof density functional (PBE)⁵¹ at the same, TZVP, basis set level. A comparison was then done between the corresponding structures obtained with the BP-86 and the PBE functionals. The comparison showed very little difference in bond lengths, angles, and dihedral values between the corresponding structures for all the cases.

A further corroboration of the small difference between the structures obtained from the two functionals comes from comparison of the potential energy surfaces for the different reactions. The ΔE values obtained from the two separate sets of DFT calculations are almost similar in most of the cases (see Tables 1–8 in the Supporting Information), thus providing further proof of the reliability of the BP-86 functional in obtaining optimized geometries and transition states. Care was taken to ensure that the obtained transition state structures possessed only one imaginary frequency corresponding to the correct normal mode.

The validity of the obtained transition states was further confirmed by doing IRC⁵² calculations: the correct reactant and product structures were obtained for every transition state obtained. To do the IRC calculations, Turbomole 6.4 was employed. Subsequent to obtaining the reliable optimized minima and transition states as discussed here, single-point calculations were performed with the hybrid B3-LYP functional^{53,54} to obtain more reliable energy values for the potential energy surfaces for the different investigated reactions. Solvent effects were incorporated through single-point calculations using the COSMO model,⁵⁵ with tetrahydrofuran ($\epsilon = 7.52$) as the solvent. Moreover, dispersion corrections were also included through single-point calculations. The contributions of internal energy and entropy were obtained from frequency calculations performed on the DFT structures at 298.15 K; thus, the energies reported in the figures are the ΔG values. To account for the fact that all the species are in solution, the translational entropy term in the calculated structures was corrected through a free volume correction introduced by Mammen et al.⁵⁶

It is to be noted that the entropic term is likely to be misrepresented when the reactants are considered separately in a reaction pathway. It is well-known that the translational entropy is artificially increased in such cases.⁵⁶ Though the use of the free volume correction,⁵⁶ as done in all calculations reported in the manuscript, can mitigate this problem to some

extent, it is still likely to be an issue and provide heightened values for the barriers for all the reactions. Hence, to avoid this problem, all the reaction pathways have been determined starting with the reactants having formed a complex, instead of beginning from the separated reactant species, a procedure that has also been followed by other groups.^{57–63}

■ ASSOCIATED CONTENT

📄 Supporting Information

Figures S1–S8 showing free energy surfaces and structures, as discussed in the manuscript; eight tables showing the comparison between different DFT functionals, and the xyz coordinates of all the principal structures discussed in the manuscript have been provided in the Supporting Information file. This information is available free of charge via the Internet at <http://pubs.acs.org>.

■ AUTHOR INFORMATION

Corresponding Author

*Phone: +91 20 2590 2083. Fax: +91 20 2590 2636. E-mail: k.vanka@ncl.res.in.

Notes

The authors declare no competing financial interest.

■ ACKNOWLEDGMENTS

The authors acknowledge the FP7-NMP-EU-India-2 collaborative project HYPOMAP on “New Materials for Hydrogen Powered Mobile Applications” for financial support. KV also acknowledges the Department of Science and Technology (DST) for funding. The authors are also grateful to the Centre of Excellence in Scientific Computing (COESC), NCL, Pune, for providing computational facilities. The authors also acknowledge the Multi-Scale Simulation and Modeling project (MSM) for providing financial assistance.

■ REFERENCES

- (1) Albrecht, M.; van Koten, G. *Angew. Chem., Int. Ed.* **2001**, *40*, 3750.
- (2) van der Boom, M. E.; Milstein, D. *Chem. Rev.* **2003**, *103*, 1759.
- (3) Poverenov, E.; Efremenko, I.; Frenkel, A. I.; Ben-David, Y.; Shimon, L. J. W.; Leitun, G.; Konstantinovski, L.; Martin, J. M. L.; Milstein, D. *Nature* **2008**, *455*, 1093.
- (4) Kohl, S. W.; Weiner, L.; Schwartsburd, L.; Konstantinovski, L.; Shimon, L. J. W.; Ben-David, Y.; Iron, M. A.; Milstein, D. *Science (Washington, DC, United States)* **2009**, *324*, 74.
- (5) Ahuja, R.; Punji, B.; Findlater, M.; Supplee, C.; Schinski, W.; Brookhart, M.; Goldman, A. S. *Nat. Chem.* **2011**, *167*, 167.
- (6) Gunanathan, C.; Milstein, D. *Acc. Chem. Res.* **2011**, *44*, 588.
- (7) Balaraman, E.; Gunanathan, C.; Zhang, J.; Shimon, L. J. W.; Milstein, D. *Nat. Chem.* **2011**, *3*, 609.
- (8) Weng, W.; Guo, C.; Moura, C.; Yang, L.; Foxman, B. M.; Ozerov, O. V. *Organometallics* **2005**, *24*, 3487.
- (9) Käß, M.; Friedrich, A.; Drees, M.; Schneider, S. *Angew. Chem., Int. Ed.* **2009**, *48*, 905.
- (10) Musa, S.; Romm, R.; Azerraf, C.; Kozuch, S.; Gelman, D. *Dalton Trans.* **2011**, *40*, 8760.
- (11) Vigalok, A.; Uzan, O.; Shimon, L. J. W.; Ben-David, Y.; Martin, J. M. L.; Milstein, D. *J. Am. Chem. Soc.* **1998**, *120*, 12539.
- (12) Montag, M.; Schwartsburd, L.; Cohen, R.; Leitun, G.; Ben-David, Y.; Martin, J. M. L.; Milstein, D. *Angew. Chem., Int. Ed.* **2007**, *46*, 1901.
- (13) Lewis, J. C.; Wu, J.; Bergman, R. G.; Ellman, J. A. *Organometallics* **2005**, *24*, 5737.
- (14) Gusev, D. G.; Madott, M.; Dolgushin, F. M.; Lyssenko, K. A.; Antipin, M. Y. *Organometallics* **2000**, *19*, 1734.

- (15) Koridze, A. A.; Polezhaev, A. V.; Safronov, S. V.; Sheloumov, A. M.; Dolgushin, F. M.; Ezernitskaya, M. G.; Lokshin, B. V.; Petrovskii, P. V.; Peregudov, A. S. *Organometallics* **2010**, *29*, 4360.
- (16) Denney, M. C.; Pons, V.; Hebden, T. J.; Heinekey, D. M.; Goldberg, K. I. *J. Am. Chem. Soc.* **2006**, *128*, 12048.
- (17) Marder, T. B. *Angew. Chem., Int. Ed.* **2007**, *46*, 8116.
- (18) Paul, A.; Musgrave, C. B. *Angew. Chem.* **2007**, *119*, 8301.
- (19) Liu, N.; Li, X.; Sun, H. *J. Organomet. Chem.* **2011**, *696*, 2537.
- (20) Rietveld, M. H. P.; Klumpers, E. G.; Jastrzebski, J. T. B. H.; Grove, D. M.; Veldman, N.; Spek, A. L.; van Koten, G. *Organometallics* **1997**, *16*, 4260.
- (21) Wrackmeyer, B.; Vollrath, H. *Main Group Met. Chem.* **1998**, *21*, 515.
- (22) Custelcean, R. *THEOCHEM* **2000**, *505*, 95.
- (23) Stanton, J. F.; Lipscomb, W. N.; Bartlett, R. J. *J. Am. Chem. Soc.* **1989**, *111*, 5173.
- (24) Hügler, T.; Hartl, M.; Lentz, D. *Chem.—Eur. J.* **2011**, *17*, 10184.
- (25) Dunn, N. L.; Ha, M.; Radosevich, A. T. *J. Am. Chem. Soc.* **2012**, *134*, 11330.
- (26) Coyle, E. E.; O'Brien, C. J. *Nat. Chem.* **2012**, *4*, 779.
- (27) Berkessel, A.; Adrio, J. A. *J. Am. Chem. Soc.* **2006**, *128*, 13412.
- (28) Etzenbach-Effers, K.; Berkessel, A. *Asymmetric Organocat.* **2009**, *291*, 1.
- (29) Cantillo, D.; Gutmann, B.; Kappe, C. O. *J. Am. Chem. Soc.* **2011**, *133*, 4465.
- (30) Hull, J. F.; Himeda, Y.; Wang, W.-H.; Hashiguchi, B.; Periana, R.; Szalda, D. J.; Muckerman, J. T.; Fujita, E. *Nat. Chem.* **2012**, *4*, 383.
- (31) Blaquiere, N.; Diallo-Garcia, S.; Gorelsky, S. I.; Black, D. A.; Fagnou, K. *J. Am. Chem. Soc.* **2008**, *130*, 14034.
- (32) Klinkenberg, J. L.; Hartwig, J. F. *Angew. Chem., Int. Ed.* **2011**, *50*, 86.
- (33) van der Vlugt, J. I. *Chem. Soc. Rev.* **2010**, *39*, 2302.
- (34) Enthaler, S. *ChemSusChem* **2010**, *3*, 1024.
- (35) Hartwig, J. F. *Pure Appl. Chem.* **2004**, *76*, 507.
- (36) Grey, R. A.; Pez, G. P.; Wallo, A. J. *J. Am. Chem. Soc.* **1981**, *103*, 7536.
- (37) Suarez, T.; Fontal, B. *J. Mol. Catal.* **1988**, *45*, 335.
- (38) Mukherjee, D. K.; Palit, B. K.; Saha, C. R. *J. Mol. Catal.* **1994**, *88*, 57.
- (39) Storer, R. I.; Carrera, D. E.; Ni, Y.; MacMillan, D. W. C. *J. Am. Chem. Soc.* **2006**, *128*, 84.
- (40) Nugent, T. C.; El-Shazly, M. *Adv. Synth. Catal.* **2010**, *352*, 753.
- (41) Gomez, S.; Peters, J. A.; Maschmeyer, T. *Adv. Synth. Catal.* **2002**, *344*, 1037.
- (42) Kobayashi, S.; Ishitani, H. *Chem. Rev.* **1999**, *99*, 1069.
- (43) Feller, M.; Diskin-Posner, Y.; Shimon, L. J. W.; Ben-Ari, E.; Milstein, D. *Organometallics* **2012**, *31*, 4083.
- (44) Khaskin, E.; Iron, M. A.; Shimon, L. J. W.; Zhang, J.; Milstein, D. *J. Am. Chem. Soc.* **2010**, *132*, 8542.
- (45) Ahlrichs, R.; Baer, M.; Haeser, M.; Horn, H.; Koelmel, C. *Chem. Phys. Lett.* **1989**, *162*, 165.
- (46) Becke, A. D. *Phys. Rev. A* **1988**, *38*, 3098.
- (47) Perdew, J. P. *Phys. Rev. B* **1986**, *33*, 8822.
- (48) Weigend, F. *Phys. Chem. Chem. Phys.* **2002**, *4*, 4285.
- (49) Eichkorn, K.; Treutler, O.; Oehm, H.; Haeser, M.; Ahlrichs, R. *Chem. Phys. Lett.* **1995**, *240*, 283.
- (50) Sierka, M.; Hogekamp, A.; Ahlrichs, R. *J. Chem. Phys.* **2003**, *118*, 9136.
- (51) Perdew, J. P.; Burke, K.; Ernzerhof, M. *Phys. Rev. Lett.* **1996**, *77*, 3865.
- (52) Fukui, K. *Acc. Chem. Res.* **1981**, *14*, 363.
- (53) Becke, A. D. *J. Chem. Phys.* **1993**, *98*, 5648.
- (54) Lee, C.; Yang, W.; Parr, R. G. *Phys. Rev. B* **1988**, *37*, 785.
- (55) Klamt, A. *J. Phys. Chem.* **1995**, *99*, 2224.
- (56) Mammen, M.; Shakhnovich, E. I.; Whitesides, G. M. *J. Org. Chem.* **1998**, *63*, 3168.
- (57) Kelly, E.; Seth, M.; Ziegler, T. *J. Phys. Chem. A* **2004**, *108*, 2167.
- (58) Yin, H.; Wang, D.; Valiev, M. *J. Phys. Chem. A* **2011**, *115*, 12047.
- (59) Williams, V. M.; Kong, J. R.; Ko, B. J.; Mantri, Y.; Brodbelt, J. S.; Baik, M.-H.; Krische, M. J. *J. Am. Chem. Soc.* **2009**, *131*, 16054.
- (60) Janse van Rensburg, W.; Grové, C.; Steynberg, J. P.; Stark, K. B.; Huyser, J. J.; Steynberg, P. J. *Organometallics* **2004**, *23*, 1207.
- (61) Qi, Y.; Dong, Q.; Zhong, L.; Liu, Z.; Qiu, P.; Cheng, R.; He, X.; Vanderbilt, J.; Liu, B. *Organometallics* **2010**, *29*, 1588.
- (62) Bagno, A.; Kantelechner, W.; Kress, R.; Saielli, G.; Stoyanov, E. *J. Org. Chem.* **2006**, *71*, 9331.
- (63) Li, J.-N.; Pu, M.; Ma, C.-C.; Tian, Y.; He, J.; Evans, D. G. *J. Mol. Catal. A: Chem.* **2012**, *359*, 14.